

RSC Advances



This is an *Accepted Manuscript*, which has been through the Royal Society of Chemistry peer review process and has been accepted for publication.

Accepted Manuscripts are published online shortly after acceptance, before technical editing, formatting and proof reading. Using this free service, authors can make their results available to the community, in citable form, before we publish the edited article. This *Accepted Manuscript* will be replaced by the edited, formatted and paginated article as soon as this is available.

You can find more information about *Accepted Manuscripts* in the [Information for Authors](#).

Please note that technical editing may introduce minor changes to the text and/or graphics, which may alter content. The journal's standard [Terms & Conditions](#) and the [Ethical guidelines](#) still apply. In no event shall the Royal Society of Chemistry be held responsible for any errors or omissions in this *Accepted Manuscript* or any consequences arising from the use of any information it contains.

Facile synthesis and enhanced photocatalytic activity of Sm(OH)₃ nanorods

Wang Dan, Huang Jianfeng*, Yin Lixiong, Ouyang Haibo, Li Jiayin, Wu Jianpeng

School of Materials Science & Engineering, Shaanxi University of Science and Technology, Xi'an

710021, China

Abstract: Samarium hydroxide (Sm(OH)₃) nanorods with the enhanced photocatalytic activity to degrade RhB were prepared by a facile precipitation method. The phase composition, morphology and optical properties of the as-prepared sample were characterized by X-ray diffraction, scanning electron microscopy, transmission electron microscopy and UV-vis diffuse reflectance spectroscopy. Results show that the as-prepared Sm(OH)₃ nanocrystallites are hexagonal phase with the rod-like microstructure, which exhibit strong absorption ability of UV light. Moreover, the low temperature precipitation synthesis introduced an amorphous layer on the Sm(OH)₃ nanorods. The amorphous surface layer was confirmed to have a positive impact on improving the photocatalytic activity of Sm(OH)₃ nanorods.

Keywords: Samarium hydroxide; Nanocrystalline materials; Microstructure; Photocatalytic activity

1. Introduction

Lanthanide compounds have aroused considerable interest over the past several years because of their novel optical [1], electronic [2] and chemical [3] properties arising from their 4f electrons. Lanthanide hydroxides as a kind of typical functional lanthanide compounds have caused the growing explore enthusiasm in the synthesis of one-dimensional (1D) nanostructure with the properties exploration [4–5]. A number of synthesis techniques have been developed to prepare 1D nano/microsized inorganic materials, such as hydrothermal technique [6], sol-gel route [7] and chemical conversion method [8]. Moreover, hydrothermal process [9] and homogeneous precipitation method [10] were widely used to prepare 1D lanthanide hydroxides, which may be due to their facile,

* Corresponding author: Huang J. F., Tel/Fax: +86 029 86168802

E-mail address: huangjfsust@126.com

24 high efficiency and low cost. $\text{Sm}(\text{OH})_3$ as one of the promising lanthanide hydroxides materials, the
25 hexagonal prism-like $\text{Sm}(\text{OH})_3$ nanocrystallites have been prepared for the photocatalytic degradation
26 of Rhodamine B (RhB) by hydrothermal process [11], in our previous research. To deep investigate the
27 property of $\text{Sm}(\text{OH})_3$ nanocrystallites, the facile and controllable synthesis methods will play an
28 important role in it.

29 In the present work, a low-temperature precipitation method was proposed to prepare $\text{Sm}(\text{OH})_3$
30 nanorods efficiently. Firstly, the phase composition and microstructure of the as-prepared sample were
31 investigated. Secondly, the enhanced photocatalytic activity of the sample was successfully achieved.
32 Finally, the reason for the enhanced photocatalytic activity of the as-prepared sample was analyzed.

33 2. Experiment

34 $\text{Sm}(\text{NO}_3)_3 \cdot 6\text{H}_2\text{O}$ and diethylenetriamine (DETA) were of analytical reagent (A.R.) grade and used
35 without further purification. First, 1.5 mmol $\text{Sm}(\text{NO}_3)_3 \cdot 6\text{H}_2\text{O}$ was dissolved in 60 ml distilled water,
36 then 0.28 ml DETA was added dropwise with magnetic stirring to form the precursor solution. The
37 precursor solution was transferred to a 100 ml flask and thermal aging in 60 °C water-bath for 2 h after
38 stirring for 1 h. Subsequently, the product was centrifuged and washed with distilled water and
39 anhydrous ethanol for several times, finally dried in the vacuum drying oven at 60 °C for 3 h. The
40 weight of the dried product was measured through a precision balance with sensitivity of ± 0.1 mg. The
41 reaction yield was calculated to be 84.85% by Eq.(1), which means the raw materials can be fully
42 utilized in the reaction.

$$43 \quad \text{Reaction yield}(\%) = (m/m_0) * 100\% \quad (1)$$

44 Where m represents actual yield and m_0 represents theoretical yield.

45 The crystalline microstructure of the as-prepared powder was characterized by a powder X-ray
46 diffraction (XRD, Rigaku D/max-2000) with Cu K α radiation ($\lambda=0.15406$ nm) at 40 kV and 40 mA in
47 the 2θ range of 10°~60°. The morphology of the sample was observed by field emission scanning
48 electron microscopy (FE-SEM, Hitachi S-4800, Acceleration voltage: 3 kV). High-resolution
49 transmission electron microscopy (HRTEM operated at 200 kV) was taken by field emission

50 transmission electron microscopy (FE-TEM, American FEI Tecnai G² F 20 S-TWIN). UV-vis diffuse
51 reflectance spectrum of the sample was measured by Shimadzu UV-2450 UV-vis spectrophotometer.

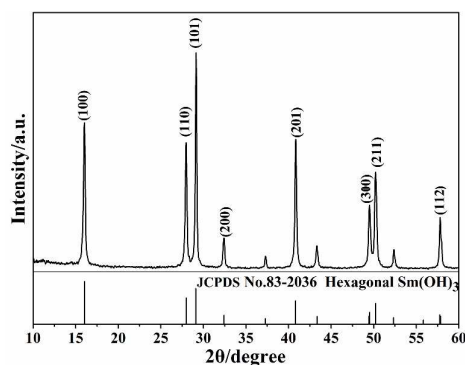
52 Photocatalytic activities of the prepared Sm(OH)₃ nanorods were evaluated by photocatalytic
53 degradation of 5 mg·L⁻¹ Rhodamine B, Methyl orange and Neutral red aqueous solution. The
54 photocatalytic activity tests were carried out by employing a BL-GHX-V photocatalytic reactor (Xi'an,
55 BILOBN, Co. Ltd.) with a 500 W mercury lamp as UV light source. The loading amount of catalysts
56 was 1.0 g·L⁻¹. Before illumination, the suspensions of dyes with catalysts were magnetically stirred in
57 the dark for 30 min, after dispersing in an ultrasonic bath for 5 min, to ensure the establishment of an
58 adsorption-desorption equilibrium between catalysts and dyes. Then, the solution was exposed to a 500
59 W mercury lamp under magnetic stirring. By the irradiation time prolong, 6 ml of the solution was
60 collected by centrifugation each 5 min. The concentrations of the remnant dyes in the collected solution
61 were monitored by UV-vis spectroscopy (Unico UV-2600) at 553 nm [11]. In the process of
62 photocatalytic reaction, the degradation efficiency of dyes was calculated by Eq. (2):

$$63 \quad \text{Degradation efficiency (\%)} = (1 - C_t/C_0) * 100\% \quad (2)$$

64 Where C₀ represents the initial concentration of dye aqueous solution and C_t represents the
65 concentration of dye aqueous solution after different minutes of UV irradiation.

66 3. Results and discuss

67 3.1. Phase analysis



68

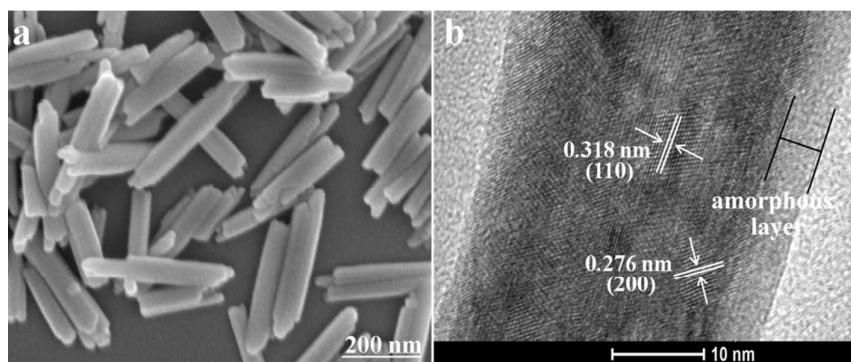
69

Fig.1. XRD pattern of the as-prepared Sm(OH)₃ nanocrystallites

70 The XRD pattern of the sample prepared by a facile precipitation method is shown in Fig.1. The
71 XRD peaks of the as-prepared sample can be finely indexed to the hexagonal $\text{Sm}(\text{OH})_3$ (JCPDS
72 No.83-2036). No characteristic peaks of impurities can be detected, indicating that the pure phase of
73 $\text{Sm}(\text{OH})_3$ was achieved under the current synthetic condition.

74 3.2. Morphological analysis

75 Fig.2 (a) shows the SEM image of the $\text{Sm}(\text{OH})_3$ nanocrystallites prepared by a facile precipitation
76 method. It can be obviously observed that the microstructure of the prepared sample is rod-like and the
77 average length of the nanorods is about 300 nm. Fig.2 (b) exhibits the high magnification TEM image
78 of an individual $\text{Sm}(\text{OH})_3$ nanorod. The lattice spacing of $d_{(200)}=0.276$ nm and $d_{(110)}=0.318$ nm were
79 clearly observed from Fig.2 (b), which means that the prepared $\text{Sm}(\text{OH})_3$ nanorods are polycrystal. The
80 $\text{Sm}(\text{OH})_3$ nanorods may be composed by numerous $\text{Sm}(\text{OH})_3$ crystalline subunits with various
81 orientations. Moreover, the high magnification TEM image of an individual $\text{Sm}(\text{OH})_3$ nanorod shows
82 that the prepared $\text{Sm}(\text{OH})_3$ nanorods were wrapped with a layer of amorphous particles. The layer of
83 amorphous particles was only found on the $\text{Sm}(\text{OH})_3$ nanorods prepared by precipitation method, by
84 comparing with the high-resolution TEM image (Fig.S1b) of the well crystallized $\text{Sm}(\text{OH})_3$ nanorods
85 prepared by hydrothermal method.

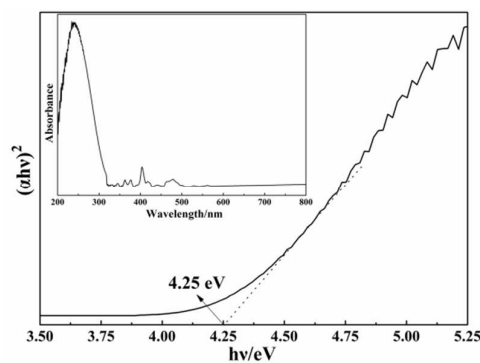


86
87 Fig.2. SEM (a) and HRTEM (b) image of the as-prepared $\text{Sm}(\text{OH})_3$ nanocrystallites

88 3.3. Optical and photocatalytical properties

89 UV-vis diffuse spectroscopy was used to characterize the optical absorbance of the as-prepared
90 $\text{Sm}(\text{OH})_3$ nanorods. Fig.3 presents the direct band-gap energy estimated from a plot of $(\alpha h\nu)^2$ vs. photo

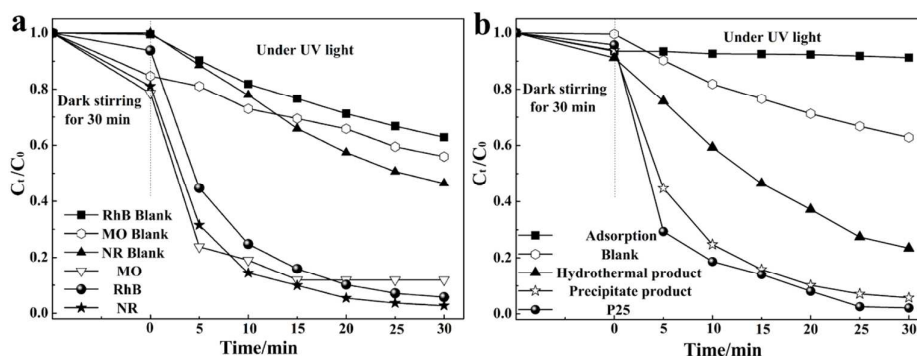
91 energy ($h\nu$) according to the K–M model. The optical band-gap of $\text{Sm}(\text{OH})_3$ nanorods is calculated to
92 be 4.25 eV. Moreover, the UV–vis diffuse spectroscopy of the as–prepared $\text{Sm}(\text{OH})_3$ nanorods is
93 shown in Fig.3(Inset), in which $\text{Sm}(\text{OH})_3$ nanorods exhibit the strong band edge absorption in the
94 region between 200–300 nm. Combine the good ultraviolet absorbing property and the unique
95 properties of lanthanide compounds [1–3], the photocatalytic activity of $\text{Sm}(\text{OH})_3$ nanorods was
96 investigated [12].



97
98 Fig.3. The relationship between $(\alpha h\nu)^2$ and photonenergy (Inset: UV–vis diffuse reflectance
99 spectrum of $\text{Sm}(\text{OH})_3$ nanorods)

100 The degradation of Rhodamine B (RhB), Methyl orange (MO), Neutral red (NR) were used to
101 evaluate the photocatalytic activity of the as–prepared $\text{Sm}(\text{OH})_3$ nanorods, corresponding
102 photocatalytic results were shown in Fig.4(a). The photocatalytic results exhibit that $\text{Sm}(\text{OH})_3$
103 nanorods can mainly degrade RhB and Neutral red in only 30 min, which degradation efficiency
104 reaches 94.3% and 97.3%, respectively. This means the prepared $\text{Sm}(\text{OH})_3$ nanorods have good
105 responsiveness to the cationic (RhB) and neutral (Neutral red) dyes. However, the degradation of
106 Neutral red is also very quick without photocatalysts, which affect the proper evaluation of the as–
107 prepared $\text{Sm}(\text{OH})_3$ nanorods. Therefore, the degradation of RhB was used to compare the
108 photocatalytic activity of the as–prepared $\text{Sm}(\text{OH})_3$ nanorods with other products.

109 The photocatalytic results of RhB degraded by different kinds of photocatalysts were shown in
 110 Fig.4(b). The adsorption test shows that the adsorption–desorption equilibrium between $\text{Sm}(\text{OH})_3$
 111 nanorods and RhB was achieved after the dark stirring for 30 min. The blank test demonstrates that the
 112 degradation of RhB is very slow without photocatalysts. When the prepared $\text{Sm}(\text{OH})_3$ nanorods were
 113 used as photocatalyst, the RhB absorption peak decreases quickly (Fig.S2.) as irradiation time prolongs.
 114 The photocatalytic results exhibit that the as–prepared $\text{Sm}(\text{OH})_3$ nanorods can mainly degrade RhB in
 115 only 30 min with the degradation efficiency reaches 94.3%. Whereas, the degradation efficiency of the
 116 fully crystallized $\text{Sm}(\text{OH})_3$ nanocrystallites prepared by hydrothermal process only reaches 76.5%.
 117 These results show that the $\text{Sm}(\text{OH})_3$ nanorods prepared by precipitation method exhibit enhanced
 118 photocatalytic activity to degrade RhB.



119 Fig.4. (a) Photocatalytic results of RhB, MO and NR degraded by $\text{Sm}(\text{OH})_3$ nanorods

120 (b) Photocatalytic results of RhB degraded by different kinds of photocatalysts

121 The microstructures and sizes of the precipitation and hydrothermal products are similar (Fig.S3.).
 122 The better photocatalytic activity of the $\text{Sm}(\text{OH})_3$ nanorods prepared by precipitation method may be
 123 due to the amorphous particles wrapped on the $\text{Sm}(\text{OH})_3$ nanorods. The functionalized surface seems to
 124 enhance the adsorption amount of dissolved oxygen and RhB molecules. This made the life–time of the
 125 photogenerated holes prolong, which can participate in the degradation process by the formation of
 126 reactive radicals or by the direct oxidation of the pollutant, so as to promote the photocatalytic reaction
 127 efficiency [13]. Moreover, the degradation efficiency of RhB can reach 97.9% when the well known
 128 commercial photocatalyst P25 was used as catalyst. This means that the photocatalytic activity of the
 129

130 prepared $\text{Sm}(\text{OH})_3$ nanorods is still needs to be improved in the further exploration. The small gap
131 between the prepared $\text{Sm}(\text{OH})_3$ nanorods and the well known commercial photocatalyst P25 suggests
132 that the improved $\text{Sm}(\text{OH})_3$ nanocrystallites have potential to be used as photocatalyst or co-catalyst
133 materials in the future.

134 4. Conclusion

135 In summary, pure hexagonal phase $\text{Sm}(\text{OH})_3$ nanorods have been successfully prepared by a facile
136 and efficient precipitation method at 60 °C for 2 h using $\text{Sm}(\text{NO}_3)_3 \cdot 6\text{H}_2\text{O}$ and DETA as raw materials.
137 The prepared sample exhibits high photocatalytic activity to degrade RhB, which degradation
138 efficiency reaches 94.3% under UV irradiation for 30 min. The enhanced photocatalytic activity of
139 $\text{Sm}(\text{OH})_3$ nanorods is attributed to the presence of the amorphous surface layer. The further research
140 about the photocatalytic mechanism of $\text{Sm}(\text{OH})_3$ nanocrystallites will be made in the future.

141 **Acknowledgments:** The authors are grateful to National Key Technology R&D Program (No.
142 2013BAF09B02), International Science and Technology Cooperation Project Funding of Shaanxi
143 Province (No. 2011KW-11), Innovation Team Assistance Foundation of Shaanxi Province (2013KCT-
144 06), Innovation Team Assistance Foundation of Shaanxi University of Science and Technology
145 (No.TD09-05), and Graduate Innovation Fund of Shaanxi University of Science and Technology.

146 References

- 147 [1] Wang GF, Peng Q, Li YD. *Acc Chem Res* 2011; 44: 322–332.
- 148 [2] Djerdj I, Garnweitner G, Su DS, Markus N. *J Solid State Chem* 2007; 180: 2154–2165.
- 149 [3] Van Der Kolk E, Dorenbos P. *Chem Mater* 2006; 18: 3458–3462.
- 150 [4] Xie JS, Wu QS, Zhang D, Ding YP. *Cryst Growth Des* 2009; 9: 3889–3897.
- 151 [5] Mu QY, Wang Y D. *J Alloys Compd* 2011; 509: 396–401.
- 152 [6] Zhu YC, Mei T, Wang Y, Qian YT. *J Mater Chem* 2011; 21: 11457–11463.
- 153 [7] Kuang Q, Lin ZW, Lian W, Jiang ZY, Xie ZX, et al. *J Solid State Chem* 2007; 180: 1236–1242.
- 154 [8] Jia G, You HP, Song YH, Jia JJ, Zheng YH, et al. *Inorg Chem* 2009; 48: 10193–10201.
- 155 [9] Wang X, Li YD. *Chem-Eur J* 2003; 9: 5627–5635.

- 156 [10] Zhang N, Yi R, Zhou LB, Gao GH, Shi RG, et al. *Mater Chem Phys* 2009; 114: 160–167.
- 157 [11] Wang D, Huang JF, Yin LX, Cao LY, Ouyang HB, et al. *Mater Lett* 2014; 116: 393–395.
- 158 [12] Huang JF, Wang D, Yin LX, Cao LY, Ouyang HB, et al. *J Alloys Compd* 2014; 612: 233–238.
- 159 [13] Krivec M, Segundo RA, Faria JL, Silva AMT, et al. *Appl Catal B: Environ* 2013; 140–141: 9–15.
- 160